# Residual compressive stress and intensity of infrared absorption of cubic BN films prepared by plasma enhanced chemical vapor deposition*

Yang Hang-Sheng(杨杭生)[a)†], Jin Pan-Pan(金盼盼)[a)], Xu Ya-Bo(徐亚伯)[b)], and Li Hai-Yang(李海洋)[b)]

[a)] *State Key Laboratory of Silicon Materials, Department of Materials Science and Engineering, Zhejiang University, Hangzhou* 310027, *China*
[b)] *Department of Physics, Zhejiang University, Hangzhou* 310027, *China*

(Received 7 May 2013; revised manuscript received 21 August 2013; published online 12 February 2014)

Theoretical and experimental investigations on the dependence of the intensity of infrared (IR) absorption of polycrystalline cubic boron nitride thin films under the residual compressive stress conditions have been performed. Our results indicate that the intensity of the IR absorption is proportional to the total degree of freedom of all the ions in the ordered regions. The reduction of interstitial Ar atom concentration, which causes the increase in the ordered regions of cubic boron nitride (cBN) crystallites, could be one cause for the increase in the intensity of IR absorption after residual compressive stress relaxation. Theoretical derivation is in good agreement with the experimental results concerning the IR absorption intensity and the Ar interstitial atom concentration in cubic boron nitride films measured by energy dispersion X-ray spectroscopy. Our results also suggest that the interstitial Ar is the origin of residual compressive stress accumulation in plasma enhanced cBN film deposition.

**Keywords:** infrared absorption, compressive stress, degree of freedom, interstitial atom

**PACS:** 72.80.Ey, 81.15.Gh, 32.30Bv, 61.77.jj **DOI:** 10.1088/1674-1056/23/3/037201

## 1. Introduction

Infrared (IR) absorption spectroscopy has been widely used to characterize solid compounds.[1,2] Although the emphasis in applications is often on the frequencies of spectral lines, there are cases where the intensity of relevant spectral lines plays an important role. For example, in the cubic boron nitride (cBN) films grown with the aid of inert gas ion bombardment,[3–7] the relative intensity of the absorption peak can be used to estimate the content of $sp^2$- and $sp^3$-bonded phases in the films.[8] Even so, the quantitative determination of the contents of $sp^3$- and $sp^2$-bonded BN was found to be problematic.[9–11] Recently, we also found that the intensity of transverse optical (TO) spectrum line of infrared absorption increases evidently after annealing and/or delamination-induced residual compressive stress relaxation in cBN films.[12,13] As a result, the intensity of IR absorption in nanometer polycrystalline films, especially for films under high residual compressive stress, deserves further study.

We once thought that this might be related to the density of states (DOS) of the TO phonon influenced by the residual stress. Early studies[14–17] have already shown that the peak position of phonon DOS varies with the strain (or stress). The experimental IR peak width is broadened more than the theoretical situation, suggesting that the strain is not uniform throughout the film. Thus, the phonon DOS seems to be too complicated to calculate.

In this study, we instead found that the intensity of the TO spectrum line is proportional to the total degree of freedom of all the ions in the ordered regions. Thus, the change of the intensity for the TO spectrum line of IR absorption could be ascribed to the change of the fraction of the ordered regions in crystallites, which is related to the concentration of Ar interstitial atoms, especially for cBN films prepared by argon-assisted plasma enhanced chemical vapor deposition (PECVD).

## 2. Experimental details

Cubic BN thin films were deposited on Si wafers by low-pressure inductively coupled PECVD.[17–19] The plasma was generated at 1 mTorr with an input power of 7 kW, and the substrate bias was controlled by another radio-frequency (RF) power supply with an input power of 20–100 W. Before film deposition, the reactor chamber was pre-evacuated to a base pressure below $10^{-7}$ Torr, then $H_2$ plasma and $N_2$ plasma were generated for 10 min and 30 min, respectively, to clean the substrate surface and chamber walls. Finally, the plasma gas composition was changed to Ar(20 sccm)+$N_2$(0.3–1 sccm)+$B_2H_6$(0.03–0.1 sccm)+He(0.3–0.9 sccm) for film deposition. The substrate temperature was maintained at approximately 600 K in all depositions. During post annealing of cBN films, the chamber was pre-evaluated to $10^{-7}$ Torr and then annealed at 1500 K in the $H_2$ atmosphere ($10^{-5}$ Torr) for 2–4 h. Samples were characterized ex situ using a Fourier transformed IR spectrometer (JASCO FT/IR-700) at normal incidence, and a high-voltage transmission electron micro-

*Project supported by the National Natural Science Foundation of China (Grant Nos. 50772096 and 61176051).
†Corresponding author. E-mail: hsyang@zju.edu.cn
© 2014 Chinese Physical Society and IOP Publishing Ltd 

scope (TOPCON EM 002BF) operating with an accelerating voltage of 200 kV for energy dispersion X-ray spectroscopy (EDX) whose probing diameter was 2 nm. The IR peak position was determined by fitting the spectrum with pure Lorentzian-type peak functions as described in Ref. [17]. The residual compressive stress was evaluated using the famous Stoney's equation,[11] where the substrate curvature was measured by a surface profilometer (KLA-Tenchor). In order to obtain the accurate curvature of substrate, Si wafer with a thickness of 100 μm was selected as substrate for curvature measurement.

## 3. Results and discussion

### 3.1. Distinction between two categories of phonon vibration modes

The structure of cBN thin films is polycrystalline with the crystallite size of several nanometers.[11–13] The film consists of both some ordered parts, i.e., the homogeneous parts in the interior of crystallites, and some disordered parts. By the latter we mean the regions near the crystallite boundaries, and the regions near some strongly distorted cells with interstitial foreign atoms (for example, Ar) introduced by ion bombardment.[20]

The phonon vibration modes in such a material can be divided into two distinct categories: the relatively extended modes in the ordered parts and the local modes in the disordered parts. The TO vibration modes belong to the former category.

The necessary condition for the extended modes to occur is the invariance of the equation of motion under the primitive basis vector translations. Based on this condition (together with the Born–von Karmen boundary condition), one can deduce a rule of vibration mode similar to the Bloch theorem. Let $\boldsymbol{u}_{l,\tau}$ denote the displacement from the equilibrium position of the ion (atom) specified by $\tau^+$ (or $\tau^-$) in the primitive cell specified by $l$ ($l$ is an integer). Remembering the Bloch theorem: $\psi(\boldsymbol{x}+\boldsymbol{a}_i)=\psi(\boldsymbol{x})\cdot\exp(\mathrm{i}\boldsymbol{k}\cdot\boldsymbol{a}_i)$, where $\boldsymbol{a}_i$ is one of the primitive basis vectors ($i=1, 2, 3$), we write the rule as

$$\boldsymbol{u}_{l+1,\tau}=\boldsymbol{u}_{l,\tau}\exp(\mathrm{i}\boldsymbol{q}\cdot\boldsymbol{a}_i), \tag{1}$$

where the lower index $l+1$ on the left-hand side means that one of the three integers of $l$ corresponding to $\boldsymbol{a}_i$ is added by one. Taking into account the dependence of $\boldsymbol{u}$ on time, i.e., $\boldsymbol{u}\propto\exp(-\mathrm{i}\omega t)$, we see that the vibration modes (1) have the form of lattice waves with a wave vector $\boldsymbol{q}$, and the phases in different cells are related in a relatively extended region.

Strictly speaking, the invariance condition can be satisfied only in the deep interior of a large crystal. However, the experimental IR absorption spectrum of the nano-crystalline BN film[3,4,11,20] exhibits a line in accordance with the theoretical dispersion relation (and density of states) of the TO phonon for a crystal.[14] This shows that the condition can be satisfied approximately in an interior region of the nanometer crystallite. Notably, the equation of motion for the vibration of a domain should remain practically unchanged provided that the domain is within the interior region both before and after the translation.

Obviously, not all the cells in a crystallite can take part in the extended modes. For example, the cells in the first layer of the crystallite boundary do not satisfy the necessary condition. Outside the boundary, there is either empty space or a differently oriented neighboring crystallite which interacts with the ions of the first layer cells in a different way that the interior part does. Hence, the first layer ions will vibrate with frequencies in a quite different way from those of the extended modes. Similar arguments can be applied to the immediate cells surrounding a strongly distorted cell which contains an interstitial foreign atom. All such cells are grouped into the disordered region, where the vibration modes (localized modes) are, in general, of different frequencies from that of the extended modes. Hence, the lattice wave in the ordered region cannot penetrate into the disordered region, but will be reflected or scattered back at the boundary. From the view point of energy transfer, each ordered region forms a quasi-independent subsystem.

### 3.2. Interaction of infrared radiation with the lattice vibration of an ordered region in polycrystalline film

The TO phonon modes are excited only in the ordered regions. We want first to find a theoretical formula for the absorption of infrared radiation with simultaneous excitation of TO phonons in these regions. We make use of the formulation and the notations for the quantization of lattice vibrations in Ref. [21]. The main problem we have to solve is that the ordered region is rather small.

A simple monochromatic plane electromagnetic wave is described by the vector potential

$$\boldsymbol{A}=(\boldsymbol{A}+\boldsymbol{A}^*)/2,\quad \boldsymbol{A}=\boldsymbol{A}_{\boldsymbol{k}p}\exp[\mathrm{i}(\boldsymbol{k}\cdot\boldsymbol{x}-\omega t)], \tag{2}$$

where the complex amplitude $\boldsymbol{A}_{\boldsymbol{k}p}=-\mathrm{i}(c/\omega)\boldsymbol{E}_{\boldsymbol{k}p}$, and $\boldsymbol{E}_{\boldsymbol{k}p}$ is the complex amplitude of the electric field with wave vector $\boldsymbol{k}$ and polarization $p$.

The Hamiltonian of the interaction between the phonons of an ordered region and the infrared field is expressed as[15]

$$H_{\mathrm{I}}=\sum_{l,\tau}\frac{e_\tau}{M_\tau c}\boldsymbol{A}(\boldsymbol{x}_{l,\tau})\cdot\boldsymbol{p}_{l,\tau}, \tag{3}$$

where $\boldsymbol{x}_{l,\tau}$ denotes the position vector of the ion $\tau^+$ (or $\tau^-$) in the cell $l$ (three integers), and $e_\tau$ and $M_\tau$ denote the charge and mass of the ion $\tau$. Since the wavelength of the infrared is much longer than the lattice constant, the argument $\boldsymbol{x}_{l,\tau}$ can be replaced by the position $\boldsymbol{R}_l$ of the centre of cell $l$. In view of the randomness of the ion momenta $\boldsymbol{p}$ in disordered region, the interaction between the local vibration modes and the infrared field can be neglected due to mutual cancellation of terms in the summation.

The generalized momentum is

$$\boldsymbol{p}_{l,\tau}=M_\tau\left(\frac{\mathrm{d}}{\mathrm{d}t}\right)\boldsymbol{u}_{l\tau}, \tag{4a}$$

and the displacement vector of the ion $(l,\tau)$ is

$$\boldsymbol{u}_{l,\tau}=\frac{1}{\sqrt{(N^{(\mathrm{o})}M_\tau)}}\sum_{\boldsymbol{q},\sigma}Q_{\boldsymbol{q}\sigma}\boldsymbol{e}_\tau^\sigma(\boldsymbol{q})\,\mathrm{e}^{\mathrm{i}\boldsymbol{q}\cdot\boldsymbol{R}_l}, \tag{4b}$$

where $N^{(\mathrm{o})}$ denotes the total number of cells in the ordered region, $Q_{\boldsymbol{q}\sigma}$ denotes the time-dependent canonical coordinates of the phonon of the normal mode $(\boldsymbol{q},\sigma)$, and $e_\sigma^\tau(\boldsymbol{q})$ denotes the ortho-normalized displacement vector in this mode. We deal with the optical modes for which another relation holds

$$\sqrt{M_-\boldsymbol{e}_-^\sigma}=-\sqrt{M_+\boldsymbol{e}_+^\sigma}. \tag{5}$$

Under the quantization of lattice vibration, $(\mathrm{d}/\mathrm{d}t)Q_{\boldsymbol{q}\sigma}$ is related to the creation and destruction operators $\boldsymbol{a}^*$ and $\boldsymbol{a}$, i.e.,

$$\left(\frac{\mathrm{d}}{\mathrm{d}t}\right)Q_{\boldsymbol{q}\sigma}=\mathrm{i}\sqrt{\left(\frac{\hbar\omega_\sigma(\boldsymbol{q})}{4\pi}\right)}(\boldsymbol{a}^*_{-\boldsymbol{q}\sigma}-\boldsymbol{a}_{\boldsymbol{q}\sigma}). \tag{6}$$

Substituting Eqs. (4)–(6) into Eq. (3), we obtain

$$\begin{aligned}H_{\mathrm{I}} &= \frac{e_{\mathrm{c}}\sqrt{(\hbar\omega_\sigma)}}{2\omega\sqrt{(2N^{(\mathrm{o})}M_+)}}\sum_{\boldsymbol{q},\sigma}(\boldsymbol{E}_{\boldsymbol{k}p}\cdot\boldsymbol{e}_+^\sigma)\,\mathrm{e}^{-\mathrm{i}\omega t}\\ &\times\left[\sum_l\mathrm{e}^{-\mathrm{i}(\boldsymbol{k}-\boldsymbol{q})\cdot\boldsymbol{R}_l}\right](\boldsymbol{a}^*_{\boldsymbol{q}\sigma}-\boldsymbol{a}_{-\boldsymbol{q}\sigma})+\mathrm{h.c.},\end{aligned} \tag{7}$$

where $e_{\mathrm{c}}=(e_-M_++e_+M_-)/M_-$ is a constant, and h.c. represents the Hermitian conjugate term.

Look at the square bracket in Eq. (7), where the summation of $l$ extends over the ordered region. If the ordered region is large enough ($>0.1$ mm), the square bracket would be proportional to $\delta(\boldsymbol{k}-\boldsymbol{q})$, implying the conservation of momentum $\boldsymbol{k}=\boldsymbol{q}$. Since in our films the size is only of a few nanometers, the summation is a problem.

Let us assume at first that the ordered region has the shape of a sphere with radius $s$. We choose the origin at the sphere center. Next, we define a function $f(\boldsymbol{x})$ as

$$\begin{aligned}f(\boldsymbol{x})&=1,\quad\text{for}\ \ |\boldsymbol{x}|\le s,\\ f(\boldsymbol{x})&=0,\quad\text{for}\ \ |\boldsymbol{x}|>s.\end{aligned} \tag{8}$$

Then, we can multiply each term in the square bracket by a factor $f(\boldsymbol{R}_l)$, and imagine that the lattice is extended to a sufficiently large size ($>0.1$ mm). In fact, all the terms corresponding to the lattice points outside the sphere vanish due to the factor, and the square bracket is not changed.

The function $f(\boldsymbol{x})$ can be Fourier transformed to contain components of various wave vectors $\boldsymbol{q}'$

$$f(\boldsymbol{x})=\frac{1}{(2\pi)^3}\int\varphi(\boldsymbol{q}')\,\mathrm{e}^{\mathrm{i}\boldsymbol{q}'\cdot\boldsymbol{x}}\,\mathrm{d}^3\boldsymbol{q}', \tag{9}$$

where

$$\begin{aligned}\varphi(\boldsymbol{q}') &= \int_{-\infty}^{\infty}f(\boldsymbol{x})\,\mathrm{e}^{\mathrm{i}\boldsymbol{q}'\cdot\boldsymbol{x}}\,\mathrm{d}^3\boldsymbol{x}\\ &= 4\pi\left[\frac{\sin(q's)}{q'^3}-\frac{s\cos(q's)}{q'^2}\right].\end{aligned} \tag{10}$$

This is a function of the magnitude $q'$ only. The distribution of $\varphi(q)$ is shown in Fig. 1.

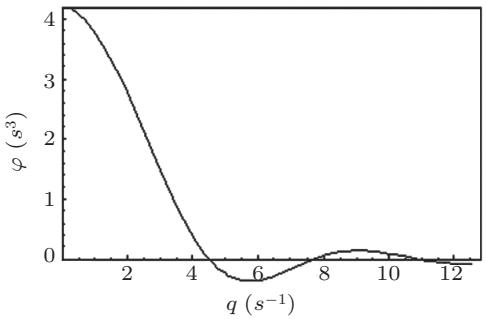



**Fig. 1.** Dependence of $\varphi$ on wave vector $(\boldsymbol{q})$.

Thus, the square bracket in Eq. (7) becomes

$$\begin{aligned}&\frac{1}{(2\pi)^3}\int\sum_{l(\text{in large region})}\mathrm{e}^{\mathrm{i}(\boldsymbol{k}-\boldsymbol{q}-\boldsymbol{q}')\cdot\boldsymbol{R}_l}\varphi(\boldsymbol{q}')\,\mathrm{d}^3\boldsymbol{q}'\\ &=\frac{1}{\Omega_{\mathrm{c}}}\int\delta(\boldsymbol{k}-\boldsymbol{q}-\boldsymbol{q}')\varphi(\boldsymbol{q}')\,\mathrm{d}^3\boldsymbol{q}'=\varphi(\boldsymbol{k}-\boldsymbol{q})/\Omega_{\mathrm{c}}.\end{aligned} \tag{11}$$

Since the wave vector of IR photon is negligibly small compared to $\boldsymbol{q}$ at the Brillouin zone boundary, $\varphi(\boldsymbol{k}-\boldsymbol{q})$ can be replaced by $\varphi(\boldsymbol{q})$. Due to the finite distribution range of $\varphi(\boldsymbol{q})$, the law of momentum conservation is violated. The range is roughly described as $|q'|<\pi/s$. If $\Delta x=2s$ and $\Delta q'=2\pi/s$, then we have $\Delta x\Delta q'=4\pi$, similar to the uncertainty principle. Thus, the violation of momentum conservation is due to the small size of the ordered region. The typical value of $s$ is about 1.5 nm, and the distribution range amounts to $2\pi/s\approx2\ \mathrm{nm}^{-1}$. This is only about 23% of the $q$ value of the boundary of Brillouin zone ($q_{\mathrm{B}}\sim8.7\ \mathrm{nm}^{-1}$). Thus, the violation is limited.

### 3.3. Absorptivity of the TO spectral line in polycrystalline film

According to the time-dependent perturbation method in quantum mechanics, the probability per unit time that a TO phonon of mode $(\boldsymbol{q},\sigma)$ is excited in an ordered region $j$ is

$$P^j_{\boldsymbol{q}\sigma}=\frac{2\pi}{h}|\langle1_{(\boldsymbol{q}\sigma)}|H^j_{\mathrm{I}}|0_{(\boldsymbol{q}\sigma)}\rangle|^2\delta(\hbar\omega-\varepsilon^j_{\mathrm{TO}}(\boldsymbol{q},\sigma)), \tag{12}$$

where $\varepsilon_{\mathrm{TO}}(\boldsymbol{q}\sigma)$ denotes the energy of a $(\boldsymbol{q}\sigma)$ TO phonon. The power of the absorption of IR radiation by the film in a thin layer of thickness $\Delta z$ and of unit area equals that of the excitation of all the TO phonons there, i.e.,

$$\begin{aligned}-\Delta I_\omega &= \sum_{j,\boldsymbol{q},\sigma}\hbar\omega P^j_{\boldsymbol{q}\sigma}\\ &= \sum_j\frac{(2\pi)^3\pi\hbar N_j^{(\mathrm{o})}e_{\mathrm{c}}^2}{4M_+V_j^{(\mathrm{o})}}\int\mathrm{d}^3\boldsymbol{q}\left(\sum_{\sigma,p}|\boldsymbol{E}_{\boldsymbol{k}p}\cdot\boldsymbol{e}_+^\sigma|^2\right)\end{aligned}$$

$$\times [\varphi_j(\boldsymbol{q})]^2 \delta(\hbar\omega - \varepsilon^j_{\rm TO}(\boldsymbol{q})), \tag{13}$$

where the summation over $j$ includes the entire ordered region inside the thin layer, and $V_j^{(\rm o)}$ denotes the volume of the ordered region in crystallite $j$.

The absorptivity $\alpha(\omega)$ of a material is defined as

$$\alpha(\omega)\Delta z = -\Delta I_\omega / I_\omega(z), \tag{14a}$$

where $I_\omega(z)$ denotes the intensity of the infrared light which may attenuate with the distance $z$

$$I_\omega(z) = \frac{c}{8\pi}\sum_p |\boldsymbol{E}_{\boldsymbol{kp}}|^2 = \frac{c}{4\pi}|\boldsymbol{E}|^2. \tag{14b}$$

The data given at the output of an FTIR spectrometer is $\alpha(\omega)t$, where $t$ is the thickness of the film. Consider the right-hand side of the following equation:

$$\alpha(\omega)t = \frac{-\Delta I_\omega t/\Delta z}{I_\omega}. \tag{15}$$

The numerator can be thought as Eq. (13) in which the field amplitude $\boldsymbol{E}$ keeps independent of $z$ and the summation over $j$ includes all the ordered regions of the film (in unit area). The denominator can be regarded as Eq. (14b) with the same field as in the numerator.

The factor $\left(\sum_{\sigma,p} |\boldsymbol{E}_{\boldsymbol{kp}} \cdot \boldsymbol{e}^\sigma_+|^2\right)$ in Eq. (13) needs some manipulation. Let the wave vector $\boldsymbol{k}$ be along the $z$ axis, and $\boldsymbol{q}$ in the direction $(\theta, \phi)$. We can choose two orthogonal and normalized TO phonon modes with vector amplitudes of positive ion as follows:

$$\boldsymbol{e}^{\rm TO1}_+ = C\frac{\boldsymbol{a}_z \times \boldsymbol{q}}{q\sin\theta}, \quad \boldsymbol{e}^{\rm TO2}_+ = C\frac{\boldsymbol{q}\times\boldsymbol{e}^{\rm TO1}_+}{q},$$

where $C = \sqrt{M_-/(M_+ + M_-)}$ and $\boldsymbol{a}_z$ denotes the unit vector along the $z$ direction. Then, the factor becomes

$$\left(\sum_{\sigma,p} |\boldsymbol{E}_{\boldsymbol{kp}} \cdot \boldsymbol{e}^\sigma_+|^2\right) = C^2|E|^2(1+\cos^2\theta).$$

From Eq. (15), we have

$$\alpha(\omega)t = \text{const.}\sum_j \frac{N_j^{(\rm o)}}{V_j^{(\rm o)2}} \langle (1+\cos^2\theta)[\varphi(\boldsymbol{q})]^2\rangle_{{\rm av},\omega} g^j_{\rm TO}(\hbar\omega), \tag{16a}$$

where const. depends on some constants ($e_{\rm c}$, $M_+$, $\pi$, $\hbar$, etc), the bracket $\langle\ \rangle_{{\rm av},\omega}$ means the average value of the argument in the $\boldsymbol{q}$ space between two equi-energy surfaces close to $\varepsilon = \hbar\omega$, and

$$g^j_{\rm TO}(\hbar\omega) = \sum_{\boldsymbol{q}\sigma} \delta(\varepsilon^{j\sigma}_{\rm TO}(\boldsymbol{q}) - \hbar\omega) \tag{16b}$$

denotes the density of states for the TO phonons at energy $\hbar\omega$.

In the extreme case where the crystallite size is very small (say, $s < 0.2$ nm, and the structure is close to amorphous), the function $\varphi(\boldsymbol{q})$ becomes nearly independent of $\boldsymbol{q}$ in the first Brillouin zone, and the bracket $\langle\ \rangle_{{\rm av},\omega}$ becomes independent of $\omega$. Then, equation (16a) implies that the absorptivity curve resembles the curve of DOS versus $\omega$ for the TO phonon.

We now turn to the typical case of cBN thin films. Since the weight function $[\varphi(\boldsymbol{q})]^2$ has a maximum at $\Gamma$ point and decreases monotonously (in the main part) with increasing $q$, the bracket $\langle\ \rangle_{{\rm av},\omega}$ should decease with increasing deviation of $\omega$ from the peak frequency $\omega_0$. Thus, the width of the absorptivity TO peak can only be smaller than (or, at most, close to) the width of the phonon DOS. The width of the TO phonon DOS for cBN was calculated to be about $6\times 10$ cm$^{-1}$ in Ref. [16]. However, the experimental absorptivity width for cBN amounts to about $2\times 10^2$ cm$^{-1}$,[3,11,13,14] and is too large to be accounted for by the theory above. People may think that this broadening can be partially ascribed to the violation of momentum conservation caused by crystalline size reduction. However, the true reason lies in that also in the calculation of phonon DOS the momentum conservation ($\boldsymbol{q} = \boldsymbol{k}$) was not taken into account. The broadening can only be ascribed to the strain or stress, which is not uniform all over the ordered regions. Since the TO peak frequency for cBN depends on stress, and shifts differently under different stress,[14,15] a broader peak can be produced via superposition.

The dependence of the TO peak frequency on stress can be calculated theoretically,[14–17] and the results of our computation and experimental measurements are shown in Fig. 2. We can estimate the range of the distribution of stress to be of order of 10 GPa. Unfortunately, except for this, we know a little more about the distribution of stress in the film. In order to avoid the unknown complicated effects of stress on the absorptivity curve, we concentrate on the integrated intensity in the next section.

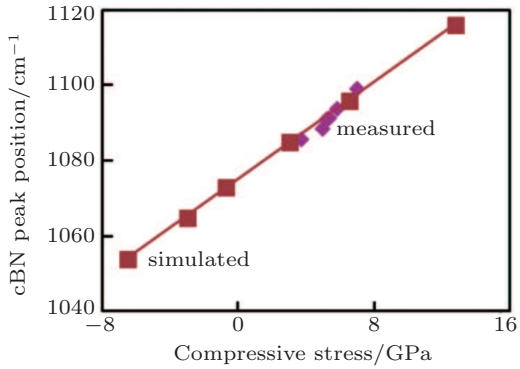



**Fig. 2.** (color online) Compressive stress induced frequency shift of IR peaks near 1080 cm$^{-1}$. Simulated data are calculated by the first-principles density-functional theory (DFT) under local density approximation (LDA).

### 3.4. Integrated intensity of a TO line in IR absorption

The integrated intensity is

$$J = \int \alpha(\omega) t \, \mathrm{d}\omega \propto \sum_j \frac{N_j^{(\mathrm{o})}}{V_j^{(\mathrm{o})2}} \int \langle (1+\cos^2)[\varphi(\boldsymbol{q})]^2 \rangle_{\mathrm{av},\omega} \times g_{\mathrm{TO}}^j(\hbar\omega)\, \mathrm{d}\omega. \quad (17)$$

Write the integral $\int f(\omega)\mathrm{d}\omega$ on the right-hand side as $\sum_i f(\omega_i)\Delta\omega_i$. The last factor $g_{\mathrm{TO}}^j(\hbar\omega_i)\Delta\omega_{\mathrm{I}}$ (multiplied by $\hbar$) equals the number of the states with energy $\hbar\omega_i$ within the interval corresponding to $\Delta\omega_i$. This, in turn, equals

$$\frac{V_j^{(\mathrm{o})}}{(2\pi)^3} \int_{\text{in region } i} \mathrm{d}^3\boldsymbol{q}_j,$$

where region $i$ means the region of the shell in $\boldsymbol{q}$ space with energy close to $\hbar\omega_i$ and shell thickness corresponding to $\Delta\omega_i$. Then, $f(\omega_i)\Delta\omega_i$ is equal to

$$\frac{V_j^{(\mathrm{o})}}{(2\pi)^3} \int_{\text{in region } i} (1+\cos^2\theta)[\varphi_j(\boldsymbol{q}_j)]^2 \mathrm{d}^3\boldsymbol{q}_j.$$

Summing over the index $i$, we change Eq. (17) into

$$J \propto \sum_j \frac{N_j^{(\mathrm{o})}}{V_j^{(\mathrm{o})}} \int_{\text{in the 1st BZ}} (1+\cos^2\theta)[\varphi_j(\boldsymbol{q}_j)]^2 \mathrm{d}^3\boldsymbol{q}_j. \quad (18)$$

Due to the limited range of the distribution of $[\varphi_j(\boldsymbol{q}_j)]^2$, the region of integration can be approximately changed to $|q| < q_n$, where $q_n$ is the $q$ value of the $n$-th zero point of $\varphi(q)$. We choose $n = 3$, so that the integration is sufficiently accurate.

When $\varphi$ depends on the magnitude $q$ only, the factor $(1+\cos^2\theta)$ can be replaced by its mean value 4/3. Then, we have

$$\int_0^{q_n} [\varphi_j(\boldsymbol{q}_j)]^2 \mathrm{d}^3\boldsymbol{q}_j = \text{const.} V_j^{(\mathrm{o})}, \quad (19)$$

where const. = 226 $\mathrm{nm}^{-3}$.

The final result is that the integrated intensity

$$J \propto \sum_j N_j^{(\mathrm{o})}, \quad (20)$$

is proportional to the total degree of freedom of all the cells in the ordered region, and is independent of the strain.

Now, we have to consider whether our previous assumption of the spherical shape of the ordered region will cause some limitations to the final result. We can assume the shape to be a cube with edge length $2s$, and follow the same deduction. Then, all the equations up to Eq. (18) remain unchanged except for the form of $\varphi(\boldsymbol{q}')$. Now, this function becomes

$$\varphi(\boldsymbol{q}') = \prod_{i=1,2,3} \varphi_i(q'_i), \quad (21)$$

where $\varphi_i(q'_i) = 2\sin(q'_i s)/q'_i$. Equation (19) remains unchanged (numerical calculation shows the same value of const.). Although in a single ordered region $\varphi_j$ depends somewhat on the direction of $\boldsymbol{q}'_j$, the random orientation of different crystallites makes $\sum_j [\varphi_j(\boldsymbol{q}'_j)]^2$ become isotropic with respect to $\boldsymbol{q}'_j$. Thus, the mean value of the factor $(1+\cos^2\theta)$ remains 4/3.

It is interesting to note that if the shape of the ordered region is assumed to be a sphere of radius $s$, with a smaller concentric sphere of radius $r_{\mathrm{d}}$ being cut off (belonging to a disordered region), the mean value of the factor $(1+\cos^2\theta)$ is still 4/3. Moreover, numerical calculation shows that equation (19) also remains practically unchanged. Anyway, the integrated intensity is by no means sensitive to the shape of ordered region, and the result (Eq. 20) holds at least approximately.

### 3.5. Interstitial Ar atoms in cBN films

In the field of cBN film deposition, high-quality cBN films can be routinely prepared.[13,18–20,22–24] However, fine controlling of the concentration of interstitial atoms (for example Ar) in a cBN film is still impossible. Fortunately, the concentration of the interstitial Ar atoms in cBN films prepared by Ar-assisted PECVD can be roughly measured using the EDX.[20] Figure 3 shows a typical EDX spectrum measured in the cBN layer from an annealed film, where peaks corresponding to B (0.19 keV), N (0.39 keV), Si (1.74 keV), C (0.28 keV), and Ar (2.95 keV) were detected. Semi-quantitative calculation reveals that the Ar:N atomic ratio is approximate to 2.8:100, which is less than that measured from the as-deposited films.[20]

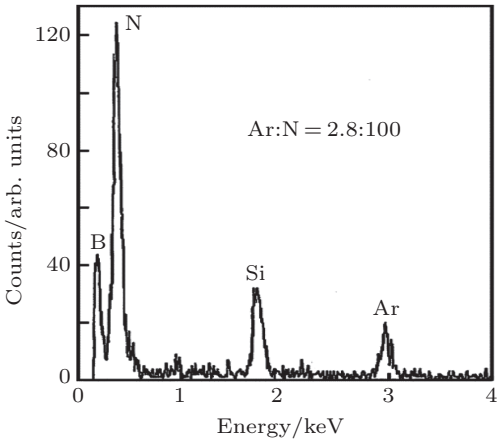



**Fig. 3.** Energy dispersion X-ray spectrum measured inside the cBN layer from a cBN film after post annealing at 1500 K in $H_2$.

Figure 4 shows the Ar:N atomic ratio of cBN films under different residual compressive stress, the atomic concentrations were measured by EDX with a probe diameter of 2 nm in the cBN layer as described in Ref. [20], and the compressive stress was evaluated from the peak shift of IR absorption

of cBN near 1080 $cm^{-1}$.[11–13,17] With the increase of interstitial Ar concentration, the IR peak position shifts to high wavenumbers accordingly, indicating the increase in residual compressive stress. Obviously, the interstitial Ar concentration is correlated with the accumulation of residual compressive stress in cBN films. Moreover, after the film was post-annealed to 1500 K in $H_2$,[13,17] the reduction of residual compressive stress is also accompanied with the decrease of interstitial Ar concentration, as the pink arrow shows in Fig. 4. This is in agreement with Reinke's results,[25,26] though stress accumulation is not a necessary parameter for cBN nucleation and growth.[17,23,27,28] These results also suggest that the interstitial Ar atom can be considered as the origin of residual compressive stress accumulation in cBN films prepared by Ar-assisted CVD.

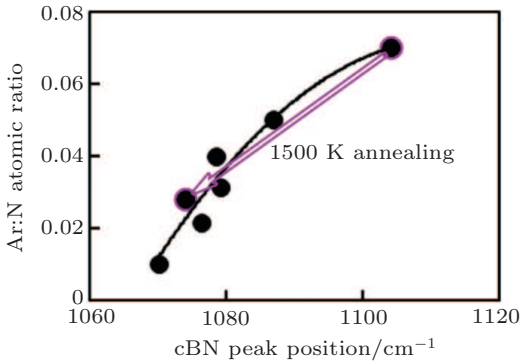



**Fig. 4.** (color online) Correlation between Ar:N atomic ratio and IR peak position of cBN. The reduction of the Ar:N ratio and the corresponding IR peak shift by 1500-K post annealing are also shown.

The effects of post annealing on the interstitial Ar atoms in BN films have been investigated using the Rutherford backscattering. Ar was found to be trapped both in the initial hexagonal BN (hBN) layer and in the upper cBN layer.[29,30] Ar in the hBN layer starts to diffuse out at relatively low annealing temperature of 1240 K. However, the Ar trapped within c-BN grains is still immobile at 1370 K, so the residual compressive stress relaxation is limited by 1370-K annealing.[29] This is in good agreement with our previous result which revealed that an annealing temperature of 1500 K is necessary to induce the release of the residual compressive stress and to promote the cBN film adhesion,[13] which seems to be attributed to the outdiffusion of interstitial Ar atoms in cBN layer as the pink arrow shows in Fig. 4.

### 3.6. Residual compressive stress and intensity of IR absorption

Recently, we have found that all the IR peak intensities of cBN films prepared by Ar-assisted PECVD are suppressed evidently by the residual compressive stress, and this suppression is reduced after post annealing or film delamination-induced stress relaxation.[11–13,17] However, the reason for the compressive stress-induced IR peak intensity change is still not yet understood. In this study, as shown in Fig. 5, the intensity of the IR peak near 1080 $cm^{-1}$ is found to almost have increased linearly with the compressive stress relaxation. For example, the IR peak intensity of cBN increases by approximately 43% with a residual compressive stress relaxation of 2.1 GPa, and the peak intensity is found to be increased up to 190% of the original intensity after 9.1-GPa stress relaxation. In summary, from Figs. 2, 4, and 5, it is evident that the intensity of IR peak of cBN film is correlated with the concentration of Ar interstitial atoms in the cBN crystallites.

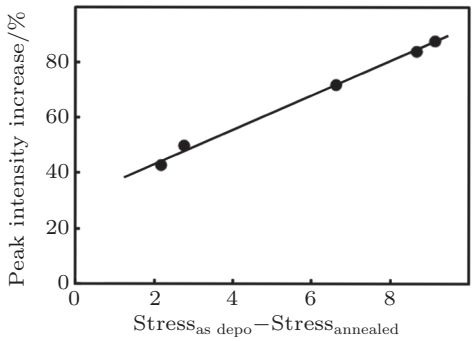



**Fig. 5.** Post annealing-induced stress relaxation and corresponding IR absorption intensity increase near 1080 $cm^{-1}$.

From Eq. (20), we can find that the increase of $J$ can only be caused by the increase of the ordered region in the cBN crystallites. While the annealing temperature is not high enough to affect the crystallite size,[13] so the increase of the ordered region in the cBN crystallites can only be explained by the release of the interstitial atoms by diffusing through the crystallite and get away when they reach the grain boundary during the annealing. Similar explanation can also be applied to the case of the delamination of cBN thin films.[12] Though the measurement of Ar concentration shown in Fig. 4 in cBN films is very difficult because of the complicated specimen preparation procedure, the reduction of Ar interstitial atoms, which increases the ordered regions of cBN crystallites, could be the reason for the increase in the intensity of IR absorption of cBN after post annealing-induced residual compressive stress release, which is in semi-quantitative agreement with our theoretical analysis

## 4. Conclusions

In summary, both our theoretical approach and experimental results reveal that interstitial atoms are introduced into cBN films during the PECVD process with Ar ion bombardment. The interstitial Ar atoms induce cBN crystallite distortion and residual compressive stress accumulation, which also reduces the fraction of the ordered regions in crystallites and thus suppresses the intensity of IR absorption. The interstitial atoms can be released effectively by post annealing. Accordingly, the suppression of IR absorption is recovered. The derived formula for the intensity of IR absorption in cBN film

can reasonably explain the stress-induced substantial change of IR peak integrated intensity.

## Acknowledgments

The authors acknowledge Prof. Toyonobu Yoshida at the University of Tokyo for sample preparation, characterization, and helpful discussion.

## References

[1] Turrell G 1972 *Infrared and Raman Spectra of Crystals* (London: Academic Press)
[2] Brodsky M H 1982 *Light Scattering in Solids I, Topics in Applied Physics* (Cardona M and Guntherodt G ed.) (vol. 8) (Berlin: Springer) p. 205
[3] Mirkarimi P B, McCarty K F and Medlin D L 1997 *Mater. Sci. Eng. R: Rep.* **21** 47
[4] Yoshida T 1996 *Diam. Relat. Mater.* **5** 501
[5] Samantaray C B and Singh R N 2005 *Int. Mater. Rev.* **50** 313
[6] Yang H S, Nie A M and Zhang J Y 2009 *Acta Phys. Sin.* **58** 1364 (in Chinese)
[7] Tian L, Ding Y, Chen H, Liu J K, Deng J X, He D Y and Chen G H 2006 *Acta Phys. Sin.* **55** 5441 (in Chinese)
[8] Friedmann T A, Mirkarimi P B, Medlin D L, McCarty K F, Klaus E J, Boehme D, Johnsen H A, Mills M J and Ottersen D K 1994 *J. Appl. Phys.* **76** 3088
[9] Jaeger S, Bewilogue K and Klages C P 1994 *Thin Solid Films* **245** 50
[10] Tsuda O, Yamada Y, Fujii T and Yoshida T 1995 *J. Vac. Sci. Technol. A* **13** 2843
[11] Yang H S, Zhang Y, Zhang X B and Xu Y B 2007 *Appl. Phys. Lett.* **91** 061907
[12] Yang H S, Zhang J Y, Nie A M and Zhang X B 2008 *Chin. Phys. B* **17** 3453
[13] Yang H S, Chen A L and Qiu F M 2011 *Diam. Relat. Mater.* **20** 1179
[14] Fahy S 1995 *Phys. Rev. B* **51** 12873
[15] Cardona M and Anastassakis E 1996 *Phys. Rev. B* **54** 14888
[16] Kern G, Kresse G and Hafner J 1999 *Phys. Rev. B* **59** 8551
[17] Liu Y, Jin P P, Chen A L, Yang H S and Xu Y B 2012 *J. Appl. Phys.* **112** 053502
[18] Yang H S, Iwamoto C and Yoshida T 2002 *Thin Solid Films* **407** 67
[19] Yang H S, Iwamoto C and Yoshida T 2007 *Diam. Relat. Mater.* **16** 642
[20] Yang H S, Iwamoto C and Yoshida T 2003 *J. Appl. Phys.* **94** 1248
[21] Callaway J 1991 *Quantum Theory of the Solid State* (London: Academic Press)
[22] Zhang X W, Boyen H G, Deyneka N, Ziemann P, Banhart F and Schreck M 2003 *Nat. Mater.* **2** 312
[23] Matsumoto S and Zhang W 2000 *Jpn. J. Appl. Phys.* **39** L442
[24] Zhang W J, Bello I, Lifshitz Y, Chan K M, Meng X, Wu Y, Chan C Y and Lee S T 2004 *Adv. Mater.* **16** 1405
[25] Reinke S, Kuhr M and Kulisch W 1996 *Diam. Relat. Mater.* **5** 508
[26] Reinke S and Kulisch W 1997 *Surf. Coat. Technol.* **97** 23
[27] Teii K, Yamao R, Tamamura T and Matsumoto S 2007 *J. Appl. Phys.* **101** 033301
[28] Teii K and Matsumoto S 2012 *ACS Appl. Mater. Interf.* **4** 5249
[29] Deyneka N, Zhang X W, Boyen H G, Ziemann P, Fukarek W, Kruse O and Möller W 2003 *Diam. Relat. Mater.* **12** 37
[30] Plass M F, Fukarek W, Kolitsch A, Schnell N, Möller W 1997 *Thin Solid Films* **305** 172